



## Original Articles

## A mechanism for spatial perception on human skin

Francesca Fardo<sup>a,b,c</sup>, Brianna Beck<sup>a</sup>, Tony Cheng<sup>d,e</sup>, Patrick Haggard<sup>a,d,\*</sup><sup>a</sup> Institute of Cognitive Neuroscience, University College London, London WC1N 3AZ, United Kingdom<sup>b</sup> Danish Pain Research Centre, Department of Clinical Medicine, Aarhus University, 8000 Aarhus, Denmark<sup>c</sup> Interacting Minds Centre, Aarhus University, 8000 Aarhus, Denmark<sup>d</sup> Institute of Philosophy, University of London, London WC1E 7HU, United Kingdom<sup>e</sup> Department of Philosophy, University College London, London WC1E 6BT, United Kingdom

## ARTICLE INFO

## Keywords:

Path integration  
Skin  
Localisation  
Space perception  
Touch  
Receptive fields

## ABSTRACT

Our perception of where touch occurs on our skin shapes our interactions with the world. Most accounts of cutaneous localisation emphasise spatial transformations from a skin-based reference frame into body-centred and external egocentric coordinates. We investigated another possible method of tactile localisation based on an intrinsic perception of ‘skin space’. The arrangement of cutaneous receptive fields (RFs) could allow one to track a stimulus as it moves across the skin, similarly to the way animals navigate using path integration. We applied curved tactile motions to the hands of human volunteers. Participants identified the location midway between the start and end points of each motion path. Their bisection judgements were systematically biased towards the integrated motion path, consistent with the characteristic inward error that occurs in navigation by path integration. We thus showed that integration of continuous sensory inputs across several tactile RFs provides an intrinsic mechanism for spatial perception.

## 1. Introduction

When you are moving around a dark room at night, without visual landmarks for identifying your position, you can nevertheless know where you are in space, by computing how you have moved around the room. For example, you could count the number of steps you take, and the direction and extent of any turns. This implicit sense of space can be built based on a mechanism of ‘path integration’, also known as ‘dead reckoning’. A large body of literature has shown that animals use self-motion information to update their current position, and to compute information about distance and direction between external locations (Mittelstaedt & Mittelstaedt, 1980). This computation is thought to be performed by ‘grid cells’ in the entorhinal cortex that encode spatial relations in a grid-like allocentric coordinate space (Doeller, Barry, & Burgess, 2010; Hafting, Fyhn, Molden, Moser, & Moser, 2005; Killian, Jutras, & Buffalo, 2012; Yartsev, Witter, & Ulanovsky, 2011). Interestingly, the mechanism of path integration is thought to mediate other functions besides navigation of external space. For instance, a recent study suggested that the human brain also uses a grid-like spatial code to organise abstract conceptual knowledge (Constantinescu, O’Reilly, & Behrens, 2016). Here, we investigated whether people may use a form of tactile path integration as a way of localising objects moving across a grid-like organisation of receptive fields (RFs) on the skin.

Historically, psychologists have thought about tactile spatial perception as involving an entirely different mechanism, in which the labelled lines of topographically organised projections in the central nervous system provide absolute location information. The question then arises of how neural activity within a particular labelled line leads to a spatial experience of ‘there-ness’. According to local sign theory (Lotze, 1884), neural activity in each nerve fibre becomes associated with an orienting movement, such as a saccade, to the corresponding location. The association with the movement is supposed to generate the spatial quality of experience (see Rose, 1999). On this view, cortical topography would allow absolute spatial location to be perceived directly, as a readout of the somatotopic map in primary somatosensory cortex (Penfield & Boldrey, 1937; Penfield & Rasmussen, 1950). However, the view that cortical topography in and of itself suffices to perceive the absolute location of a tactile stimulus seems computationally unsatisfactory and neuro-anatomically implausible. Indeed, simply propagating the topography from the receptor surface to the cortex cannot explain how we experience stimulation of a particular RF as specifying a particular spatial location. If the cortical map simply re-duplicates the spatial organisation of the receptor array, this merely shifts the problem of local sign from the skin to the brain. Moreover, neuroanatomical findings clearly show massive convergence in the somatosensory pathway. For example, studies of rapid reorganisation

\* Corresponding author at: 17 Queen Square, London WC1N 3AZ, United Kingdom.  
E-mail address: [p.haggard@ucl.ac.uk](mailto:p.haggard@ucl.ac.uk) (P. Haggard).

following amputation suggest that even SI neurons receive latent inputs from multiple digits (Buonomano & Merzenich, 1998), while neurons in SII have receptive fields covering both hands (Iwamura, Iriki, & Tanaka, 1994).

More recent findings and theories suggested that tactile spatial perception is based on a grid-like organisation of tactile RFs (Favorov, Diamond, & Whitsel, 1987; Longo & Haggard, 2011). For example, Favorov et al. (1987) showed that the topographic organisation of the feline somatosensory cortex consists of a discontinuous, mosaic-like representation of the body surface. Further, Longo and Haggard (2011) proposed that tactile size and shape perception is mediated by a ‘pixel model’, where each pixel corresponds to a RF location. On this view, the computation of tactile distance would require ‘counting’ the number of RFs in between two stimulated locations on the skin. Here, we put forward the idea that the grid-like organisation of tactile RFs supports spatial perception on the skin via a path integration mechanism. This mechanism could be thought of as counting a succession of transitions or ‘hops’ from one RF to its neighbour, together with the direction of each hop (Longo & Haggard, 2011; Nicod, 1924). We suggest that the ability to track a stimulus moving across the skin, without visual information about its location, would be based on the relative progression of the stimulus across a grid-like spatial organisation of tactile RFs on the skin. Such relative position information would allow the location of the stimulus on the receptor array to be constructed for skin space, in the same way as an animal constructs its environmental position through navigation. In support of this view, we report a series of psychophysical experiments testing the hypothesis that tactile path integration plays a role in cutaneous localisation.

A hallmark of path integration in the spatial navigation literature is a systematic inward error relative to the initial path (Etienne & Jeffery, 2004; Müller & Wehner, 1988). After roaming in the environment (e.g., when foraging), an animal usually returns home using the fastest route. The route is approximately direct; however, it is consistently deviated towards the outbound path (Fig. 1, panel A). This so-called inward bias is remarkably consistent across species and has been considered one of the key behavioural features of path integration. Building on this literature, we investigated whether the perception of continuous tactile motion also shows this characteristic marker of path integration computations (Fig. 1, panel B). To do so, we designed a tactile spatial task, where stimuli consisted of curvilinear paths (Fig. 1, panel C). The tactile paths were designed in order to include one big deviation and one small

deviation in opposite directions (e.g., ‘S’ shapes). We then instructed participants to localise an unstimulated skin location midway between the start and end points of each S-shape, irrespective of the original curvilinear path (Fig. 1, panel D). We reasoned that if participants identified the bisection point via tactile path integration, their judgements should show a systematic ‘inward error’ directed towards the greatest deviation of the S-shaped paths. In contrast, if the bisection is computed by localising the start and end points of the continuous motion stimulus on a cognitive map of absolute spatial locations, and then transforming those locations into egocentric spatial coordinates, then localisation errors would not be influenced by the S-shaped paths.

Our results showed the hallmark inward error of path integration when bisecting tactile motion paths on the skin. A series of control experiments showed that this bias could not be accounted for by variations in the spatiotopic frame of reference, task demands, spatial attention, or patterns of localisation error. Thus, we provide evidence supporting the hypothesis that the human brain tracks stimuli moving across the body surface by integrating the motion path on a grid-like, RF-based organisation of ‘skin space’, rather than computing each momentary position of the stimulus on a cognitive map of absolute spatial locations on the body.

## 2. Materials and methods

### 2.1. Participants

A total of thirty-nine healthy volunteers took part in the study. All participants gave written informed consent to participate in the study, and were right-handed by self-report. Procedures were approved by the University College London research ethics committee, and were carried out in accordance with the guidelines in the Declaration of Helsinki.

## 3. Experiment 1

### 3.1. Participants

13 healthy volunteers participated in Exp. 1 (6 females; age range = 19–32 years).

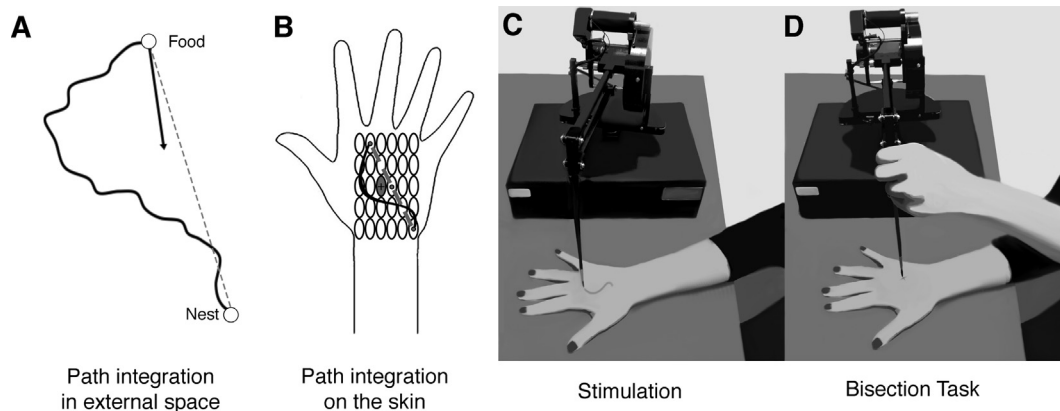


**Fig. 1.** Schematic representation of path integration in the external environment and on the skin, tactile motion stimulation, and the bisection task. (A) Example of a path in external space. The grey dashed line indicates the direct path that the animal should take to return home after foraging. The vector indicates the actual integrated path taken by the animal. This vector is deviated towards the original path to represent the typical inward error in navigation by path integration. (B) Analogous path integration hypothesis on the skin. The anisotropic circles represent the spatial organisation of tactile receptive fields on the hand dorsum, while the curvilinear black line denotes the path of a possible motion stimulus. The grey dashed line represents the direct path, while the cross indicates the bisection point, which was expected to be deviated towards the original path. This error would be consistent with the systematic inward error observed in navigation by path integration. (C) In each trial, blindfolded participants received a tactile motion stimulus on the hand dorsum via a small brush controlled by an articulated robotic arm. Participants were instructed to pay attention to the starting and ending points of the stimulus path. (D) After each stimulus, participants used the small brush to indicate the bisection point between the start and end locations of the direct path. Bisection coordinates were recorded via a button press by the experimenter.

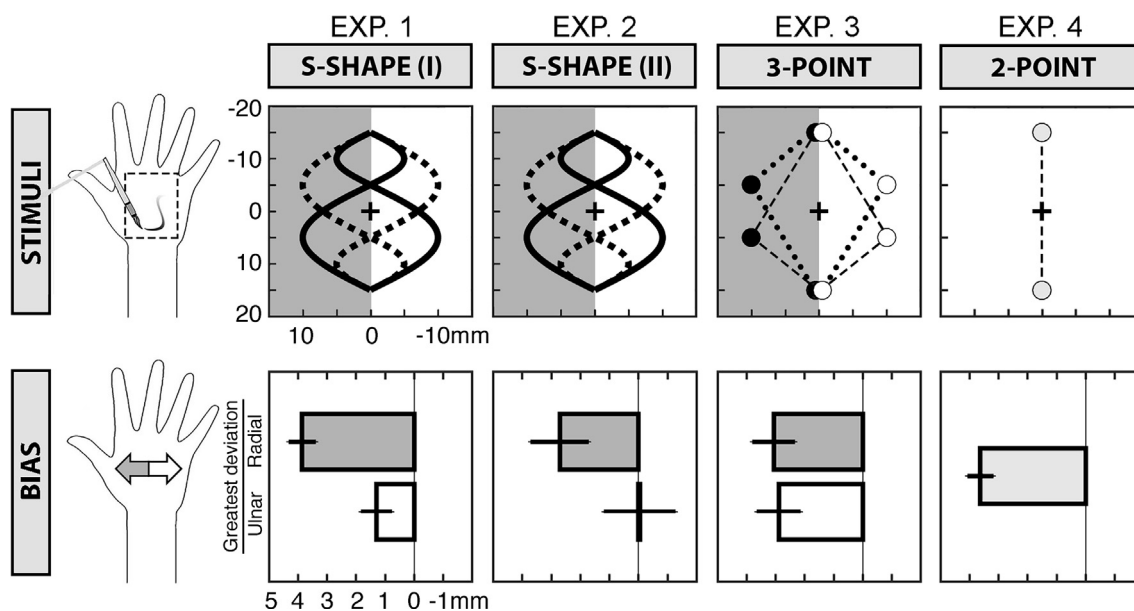


**Fig. 2.** Mean and standard error of constant localisation errors, when bisecting two reference points embedded in S-shaped (Exp. 1–2), 3-point (Exp. 3) and 2-point (Exp. 4) tactile motion stimuli. The bars show the distance of the bisection estimates, expressed in millimetres, from the actual bisection location (i.e., constant localisation error). We compared the strength of the bias as a function of the location of the greatest deviation along the radioulnar and proximodistal axes. Stimuli containing a radial or an ulnar deviation are represented in grey and white, respectively. Stimuli containing a proximal or a distal deviation are represented with full and dotted lines, respectively. In Exp. 1, the right hand was rotated 90° to the left with respect to the torso. In Exp. 2, the right hand was positioned straight-ahead from the torso.

3.2. Stimuli

Tactile stimuli consisted of continuous and curvilinear tactile motion paths. Each path was defined by two concatenated sine waves of varying widths and heights with opposite phases, forming an asymmetric S-shape. Examples of the S-shapes are depicted in Figs. 1 and 2. The start, inflection and end points of the overall S-shape were aligned along the proximodistal axis (i.e., along the hand). The inflection point was positioned either at one-third or two-thirds of the direct path between the start and the end point of each S-shape. Four families of S-shapes were defined according to the position of the biggest curve along the proximodistal and radioulnar axes. Thus, the location of the greatest curve was proximal-radial, proximal-ulnar, distal-radial, or distal-ulnar with equal probability (Fig. 2, Exp. 1–2). For each family of shapes, we generated exemplars that were systematically varied with respect to tactile motion direction (2 levels: proximal-distal, distal-proximal), start point (3 levels: -1, 0, 1 cm displacement along the proximodistal axis), angle (3 levels: -15, 0, 15 degrees rotation on the Cartesian plane) and length (2 levels: 30, 39 mm direct path length). Stimulus duration was 5 or 7 s depending on the path length. Each combination of stimulus shape, motion direction, start point, angle, and size was presented once, for a total of 144 unique stimulation trials. However, only the location of the greatest curve along the radioulnar axis was a factor of interest. Motion direction, start point, angle, and size were irrelevant to the purposes of the experiment. Motion direction was varied to counterbalance order effects, while the other factors were varied to minimise stimulus predictability. In doing so, we ensured a minimal contribution of between-trial learning, which would have contributed to the task if participants could predict the end point given the start point. Importantly, the S-shape inflection point never coincided with the mid-point, but was shifted towards either the start or the end point with equal probability. In Exp. 1, the stimuli were delivered on the dorsum of the right hand, positioned 90 degrees counter-clockwise towards the participant’s left.

3.3. Task

Participants were instructed to perform a tactile bisection task, which consisted of identifying the mid-point between the start and the end locations of each curvilinear S-shape, while ignoring the intermediate stimulation.

3.4. Procedure

Participants completed four blocks of trials, each including 36 stimuli, while blindfolded. Stimuli were delivered on the dorsum of the right hand using a small brush (2mm width) attached to a programmable robotic arm (PHANTOM Premium 1.5 haptic device, Geomagic, USA). The position of the robotic arm was controlled in MATLAB using the OpenHaptics toolkit 3.1 (Geomagic, USA) and Prok.Phantom software (Prokopenko, 2012). After each stimulation trial, participants mentally traced the direct route between the two reference points (the first and last points of stimulation) and located the mid-point of the direct path. Participants provided the bisection judgements with their left hand, by moving and positioning the tip of the robotic arm in the location corresponding to the bisection point. For each judgement, Cartesian coordinates corresponding to the position of the robotic arm were recorded via a button press by the experimenter. To ensure that the bisection judgements exclusively relied on tactile motion cues, in the absence of informative visual or proprioceptive inputs, participants were blindfolded and were not allowed to move their hand within each block of trials.

4. Experiment 2

4.1. Participants

5 healthy volunteers from Exp. 1 returned to participate in Exp. 2 (3 females; age range = 22–32 years).

## 4.2. Stimuli, task and procedure

The stimuli, task, and procedure were identical to Exp. 1, with the only exception of the hand position, which was straight-ahead rather than positioned 90 degrees counter-clockwise towards the left. The hand location with respect to the torso was rotated in space to rule out possible spatiotopic effects. Importantly, these participants received the same S-shaped tactile motion stimuli as in Exp. 1, but in a different randomised order.

## 5. Experiment 3

### 5.1. Participants

A separate group of 13 healthy volunteers participated in Exp. 3 (7 females; age range = 19–33 years).

### 5.2. Stimuli

Participants received 3-point discrete tactile motion stimuli. The three points corresponded to the start point, deviation point (corresponding to the peak of the greatest curve), and end point of each S-shape presented in Exp. 1–2. The 3-point stimuli critically differed from the S-shape with respect to the lack of continuous stimulation between the two reference points to bisect. Spatial locations and temporal delays were otherwise identical between continuous S-shapes and the three discrete points. The stimuli were delivered on the dorsum of the right hand, positioned 90 degrees counter-clockwise towards the left.

### 5.3. Task

Participants were instructed to perform a tactile bisection task, which consisted of identifying the mid-point between the start and the end locations of each discrete motion path, while ignoring the intermediate point-like stimulation.

### 5.4. Procedure

The procedure was identical to Exp. 1. This control experiment ensured that the path integration effect was present when bisecting continuous, but not discrete, tactile motion paths.

## 6. Experiment 4

### 6.1. Participants

A separate group of 13 healthy volunteers participated in Exp. 4 (10 females; age range = 18–35 years).

### 6.2. Stimuli

Participants received 2-point stimuli defined by the start point and end point of each S-shape in Exp. 1–2. The 2-point stimuli critically differed from the 3-point stimuli with respect to the lack of irrelevant tactile stimulation, while preserving identical temporal delays and spatial locations. The stimuli were delivered on the dorsum of the right hand, positioned 90 degrees counter-clockwise towards the left, as in Exp. 1 and 3.

### 6.3. Task

Participants were instructed to bisect the two stimulated skin locations.

## 6.4. Procedure

The procedure was identical to Exp. 1. This control experiment demonstrated that single-point localisation biases (e.g., radial bias) were independent from the path integration bias (i.e., inward error towards the greatest deviation of the curve).

## 6.5. Analysis

Within each experiment, we analysed the average distance between the judgement and the target in the tactile bisection task. The target corresponded to the mid-point between the first and last tactile locations in each stimulation trial and was always an unstimulated skin location. The discrepancies between expected and estimated bisection correspond to constant errors and are informative about localisation biases. In all analyses, we assessed the constant radioulnar and proximodistal errors. To this aim, we normalised (i.e., translated and rotated) all stimuli and judgements into a common spatial frame where the target location corresponded to the origin of the axis. Thus, any deviation from the origin coordinates (0,0) simply reflected the distance in millimetres from the target location. To assess whether constant localisation errors were significantly influenced by the location of the greatest path deflection, we compared judgements corresponding to radial vs. ulnar trials, as well as proximal vs. distal trials, using two paired samples t-tests for each experiment (Exp. 1–3). Finally, we assessed the strength of the localisation bias in Exp. 4 by applying a one-sample t-test to determine whether the bias was significantly different from zero. In a second analysis, we analysed the bias towards the greatest path deflection. We thus recoded the bisection judgements as positive when they were shifted towards the greatest path deflection, but negative when they were shifted away from the greatest path deflection. We used an independent samples t-test to compare the overall bias between Exp. 1 and 3.

We used a similar pipeline to analyse the variable error, which reflects the precision of localisation (i.e., standard deviation of bisection judgements). In the variable error analysis, we replicated previous findings reflecting the anisotropy of tactile RFs on the hand dorsum (i.e., larger variable errors along the proximodistal vs. radioulnar axis) and showed that radioulnar and proximodistal variable errors were not influenced by path integration.

## 7. Results

### 7.1. The magnitude of radioulnar errors is influenced by tactile path integration within a somatotopic frame of reference

In Exp. 1 (S-shapes), participants' bisection judgements were biased towards the greatest arc of the S-shape ( $t(12) = 6.20$ ,  $p < 0.001$ , Cohen's  $d_z = 1.72$ ; Figs. 2 and 4). In addition, there was an overall bias to make bisection errors towards the radius. Crucially, this bias was stronger when the major arc of the S-shape was towards the radial direction ( $M = 3.86$ ,  $SD = 1.70$  mm), than when the major arc was towards the ulnar direction ( $M = 1.30$ ,  $SD = 1.95$  mm). Thus, although there was an overall radial bias in localisation, this bias was consistently modulated by the direction of the greatest deviation along the path. This modulation conforms to the typical inward error in navigation tasks (Etienne & Jeffery, 2004; Müller & Wehner, 1988). We obtained similar results in Exp. 2 (S-shapes), in which the hand was oriented with the fingers pointing away from the torso ( $t(4) = 5.04$ ,  $p < 0.01$ , Cohen's  $d_z = 2.26$ ; Figs. 2 and 4), rather than parallel to the torso as in Exp. 1. Again, the bias was stronger when the major arc of the S-shape was towards the radial direction ( $M = 2.71$ ,  $SD = 2.24$  mm), than when the major arc was towards the ulnar direction ( $M = -0.04$ ,  $SD = 2.76$  mm). These results suggest that the bias towards the large arc depends on the stimulation pattern on the skin, and is largely independent of the egocentric spatial frame and the

organisation of the motor response used to express localisation judgements.

In Exp. 3 (3-point stimuli), we confirmed that this effect was specific to continuous path integration, as there was no systematic constant error in bisection towards the intermediate point in a series of three discrete single-point stimuli ( $t(12) = 0.53$ ,  $p = 0.60$ , Cohen's  $d_z = 0.15$ ; Figs. 2 and 4). Indeed, the bias was similar irrespective of the location of the intermediate point towards the radial direction ( $M = 3.07$ ,  $SD = 2.68$  mm) or the ulnar direction ( $M = 2.90$ ,  $SD = 2.74$  mm). This result excluded the possibility that bisection bias was a simple by-product of shifting exogenous spatial attention to one side of the start-end axis – the stimulation centre of mass in fact shifts farther from the start-end axis in a 3-point series than in the S-shaped paths. Finally, in Exp. 4 (2-point stimuli), we confirmed the overall radial bias of Exp. 1, and showed that it was independent of any intermediate path, since it occurred when simply bisecting two discrete stimulated points ( $M = 3.63$ ,  $SD = 1.64$  mm;  $t(12) = 7.98$ ,  $p < 0.001$ , Cohen's  $d = 2.21$ ; Figs. 2 and 4). These results suggest an overall radial bias component, independent of the effect of the intermediate path, but consistent with previous reports of single-point localisation on both the palm (Culver, 1970) and the hand dorsum (Mancini, Longo, Iannetti, & Haggard, 2011).

### 7.2. Bias towards the greatest path deflection

In a second analysis, we calculated the bias towards the greatest deviation, irrespective of the somatotopic frame of reference. We expressed each bisection judgement as positive when it was towards the greatest deviation, but negative when it was away from the greatest deviation, irrespective of its radial or ulnar location. We then averaged and analysed the bisection judgement values. In doing so, we isolated a path integration-specific bias component that was independent from other sources of localisation error such as overall radial bias. A significant positive or negative average would suggest a significant bias towards or away from the greatest path deflection, respectively. Instead, a value of zero would suggest lack of directional bias towards or away from the greatest path deflection, while controlling for other path-unrelated localisation errors. One sample t-tests demonstrated a positive bias towards the greatest path deflection when participants judged continuous S-shapes ( $t(12) = 6.20$ ,  $p < 0.001$ , Cohen's  $d = 1.72$ ;  $M = 1.28$ ,  $SD = 0.74$  mm), but no significant bias around zero when participants bisected 3-point stimuli ( $t(12) = 0.53$ ,  $p = 0.60$ , Cohen's  $d = 0.15$ ;  $M = 0.08$ ,  $SD = 0.57$  mm). Crucially, the difference in bias between continuous paths and 3-point stimuli was significant ( $t(24) = 4.58$ ,  $p < 0.001$ , Cohen's  $d = 1.80$ ; Fig. 3). In summary, the systematic mislocalisation towards the point of maximal deviation in a continuous intermediate path is consistent with the characteristic inward error in navigation by path integration (Exp. 1). This mislocalisation was independent of the spatiotopic frame of reference (Exp. 2), exogenous spatial attention (Exp. 3) and general tactile localisation biases (Exp. 4).

### 7.3. The magnitude of proximodistal errors is influenced by tactile path integration

In Exp. 1, participants' bisection judgements were also significantly biased towards the greatest arc of the S-shape along the proximodistal axis ( $t(12) = 2.71$ ,  $p = 0.02$ , Cohen's  $d_z = 0.75$ ). However, the effect size of the proximodistal displacement was smaller than the effect size of the radioulnar displacement (Cohen's  $d_z = 0.75$  vs.  $d_z = 1.72$ ). The overall bias in the bisection judgements was towards the fingers (i.e., distal location). However, the bias was stronger when the major arc of the S-shape was towards the proximal direction ( $M = -0.11$ ,  $SD = 3.11$  mm), than when the major arc was towards the distal direction ( $M = -1.04$ ,  $SD = 2.61$  mm). Instead, in Exp. 2, we did not replicate the proximodistal effect ( $t(4) = -0.61$ ,  $p = 0.57$ , Cohen's

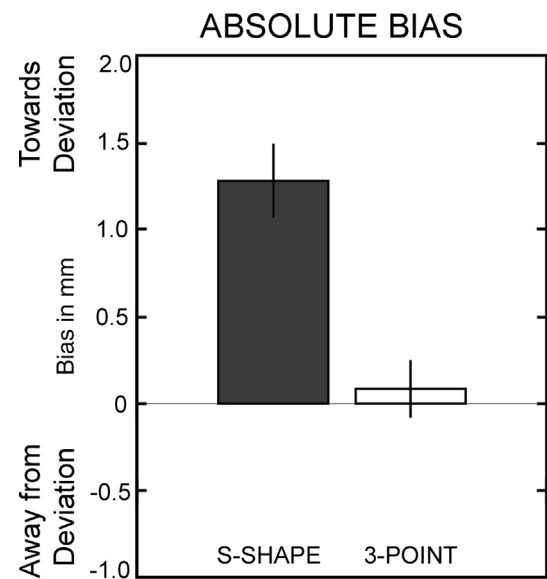


Fig. 3. Mean and standard error of the absolute constant localisation errors in Exp. 1 (S-shape) and Exp. 3 (3-point). Positive values indicate a bias towards the greatest deviation, while negative values indicate a bias away from the greatest deviation. The localisation bias was significantly shifted towards the convexity (i.e., greatest deviation) when the path was continuous (S-shape), whereas no bias was found when the path consisted of three discrete points (3-point).

$d_z = -0.27$ ). Participants' judgements were biased towards the distal location, but the strength of the bias was not modulated by the position of the greatest deflection (proximal:  $M = 0.34$ ,  $SD = 3.77$  mm; distal:  $M = 0.79$ ,  $SD = 2.92$  mm). It is important to note that we used a power analysis to identify a sufficient number of participants to replicate only the radioulnar effect in Exp. 2 (i.e.,  $N = 5$  participants). As a consequence, we did not have enough power to draw any conclusions about whether the bias along the proximodistal axis was influenced by the spatial frame of reference.

In Exp. 3, there was no systematic proximodistal constant error in bisection towards a single intermediate point in a discontinuous 3-point series ( $t(12) = 1.57$ ,  $p = 0.14$ , Cohen's  $d_z = 0.44$ ). Indeed, the bias was similar irrespective of the location of the intermediate point towards the proximal direction ( $M = 0.01$ ,  $SD = 3.34$  mm) or the distal direction ( $M = -0.50$ ,  $SD = 3.89$  mm). Thus, we excluded the possibility that the proximodistal bias in Exp. 1 was a simple by-product of shifting exogenous spatial attention to one side of the start-end axis. Finally, in Exp. 4 (2-point stimuli), we found that participants had no systematic localisation error along the proximodistal axis. Indeed, the judgements were not significantly different from zero ( $M = 0.33$ ,  $SD = 3.62$  mm;  $t(12) = 0.33$ ,  $p = 0.75$ , Cohen's  $d = 0.09$ ). These results suggest a weaker distal bias component, modulated by the intermediate continuous path, but not by distracting intermediate point-like stimuli, in a similar fashion as for the radioulnar bias. Although we did not observe a clear distal bias in tactile bisection of two-point stimuli, large distal biases have been previously reported in single-point tactile localisation on the hand dorsum (Mancini et al., 2011; Margolis & Longo, 2015). This discrepancy could be related to task-specific factors (e.g., bisection vs. single-point localisation).

### 7.4. The precision of radioulnar and proximodistal errors is not influenced by tactile path integration

The variability of the bisection judgements (i.e., variable error) was independent from the radioulnar and proximodistal location of the larger S-shape deflection. In Exp. 1, participants' bisection judgements had similar precision, irrespective of the greatest deflection of the S-

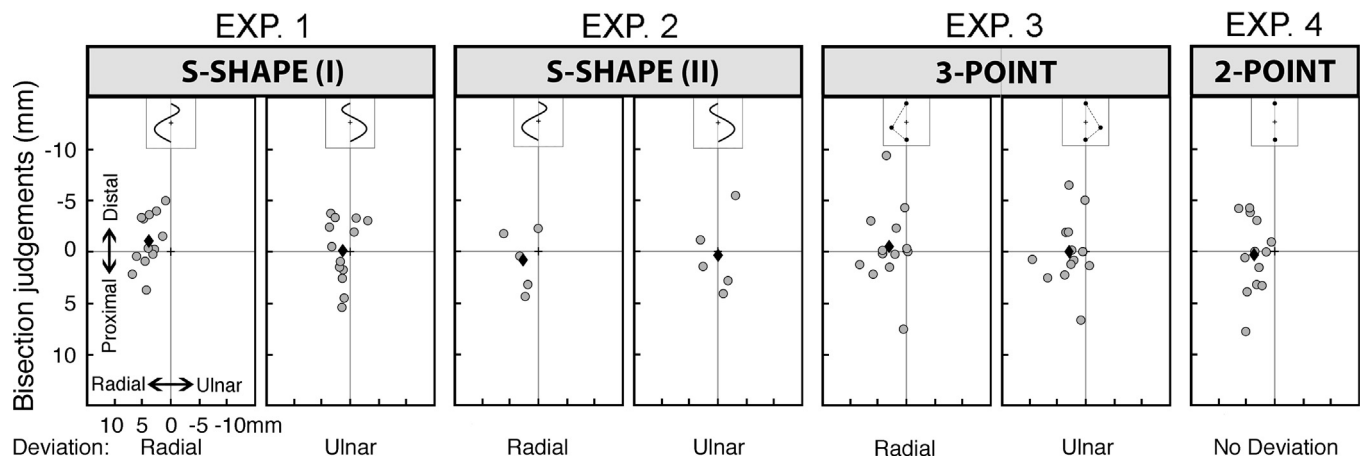


**Fig. 4.** Constant localisation errors (i.e., location of the bisection judgements in mm), shown separately for radial and ulnar deviation locations. The grey dots represent single-subject averages, while the black diamonds correspond to group averages. Bisection judgements were biased towards the greatest deviation when stimuli were continuous S-shapes (Exp. 1–2), but not when the deviation consisted of a single intermediate point (Exp. 3). The two-point bisection task (Exp. 4) confirmed that the radial bias was independent of the manipulation of continuous and discrete intermediate stimulation.

shape along the radioulnar ( $t(12) = -0.74$ ,  $p = 0.47$ , Cohen's  $d_z = -0.20$ ) and the proximodistal axes ( $t(12) = -0.05$ ,  $p = 0.96$ , Cohen's  $d_z = -0.01$ ). Localisation precision was not modulated by the position of the greatest deflection towards the radial direction ( $M = 4.52$ ,  $SD = 0.91$  mm) or the ulnar direction ( $M = 4.63$ ,  $SD = 0.99$  mm). Similarly, localisation precision did not vary when the greatest deflection was towards the proximal direction ( $M = 6.74$ ,  $SD = 1.37$  mm) or the distal direction ( $M = 6.75$ ,  $SD = 1.47$  mm). Likewise, in Exp. 2, the precision of bisection judgements did not differ with respect to the location of the greatest path deflection across the radioulnar axis ( $t(4) = -2.70$ ,  $p = 0.05$ , Cohen's  $d_z = -1.21$ ) or along the proximodistal axis ( $t(4) = 1.52$ ,  $p = 0.20$ , Cohen's  $d_z = 0.68$ ). Again, localisation precision was not modulated by the position of the greatest deflection towards radial ( $M = 4.04$ ,  $SD = 0.89$  mm), ulnar ( $M = 4.48$ ,  $SD = 0.69$  mm), proximal ( $M = 6.43$ ,  $SD = 1.35$  mm), or distal ( $M = 5.84$ ,  $SD = 0.60$  mm) directions.

Interestingly, in Exp. 3, the precision of bisection judgements varied across the radioulnar axis ( $t(12) = -2.31$ ,  $p = 0.04$ , Cohen's  $d_z = -0.64$ ), but not along the proximodistal axis ( $t(4) = -0.49$ ,  $p = 0.63$ , Cohen's  $d_z = -0.14$ ). When bisecting 3-point stimuli, bisection judgements were more precise when the intermediate point to ignore was towards the radial direction ( $M = 4.66$ ,  $SD = 1.08$  mm) rather than the ulnar direction ( $M = 5.03$ ,  $SD = 1.13$  mm). However, similar variability was observed when the intermediate point to ignore was towards the proximal direction ( $M = 7.87$ ,  $SD = 1.20$  mm) compared to the distal direction ( $M = 8.01$ ,  $SD = 1.42$  mm). Finally, in Exp. 4, we observed that localisation precision was of similar magnitude as in the previous experiments both across the radioulnar axis ( $M = 4.41$ ,  $SD = 1.07$  mm) and along the proximodistal axis ( $M = 7.75$ ,  $SD = 1.39$  mm).

Across all four experiments, the precision of bisection judgements was greater along the radioulnar axis than the proximodistal axis. These results are consistent with previous studies in tactile localisation biases and tactile distance perception on the hand dorsum, which found that single-point localisation accuracy (Schlereth, Magerl, & Treede, 2001) and precision (Margolis & Longo, 2015) were greater in the radioulnar axis than the proximodistal axis. Further, tactile distance was perceived as longer when two tactile stimuli were across vs. along the hand (Longo & Haggard, 2011). Altogether, these findings can be attributed to the spatial acuity of tactile RFs, which is directly related to their specific elongated morphology. Indeed, the precision of localisation, as well as the precision of distance perception, can be simply explained by the anisotropy of tactile RFs, with increased variability in localisation along the elongated direction (i.e., proximodistal).

## 8. Discussion

Our results are consistent with a process of tactile path integration that constructs a RF-based organisation of 'skin space', from which the location of a stimulus moving across the body surface can be computed. We quantified the perception of spatial distances on the skin using a bisection task of curved tactile motion stimuli, and instructing participants to identify an unstimulated skin location midway between the start and end points of each stimulation trial. This technique isolated a bias in tactile spatial localisation that was specifically related to the integration of continuous tactile motion cues, and was consistent with the hallmark inward error of path integration, i.e., a displacement towards the integrated path (Etienne & Jeffery, 2004; Müller & Wehner, 1988). Importantly, in a series of control experiments, we showed that the inward error was not influenced by changes in the spatiotopic frame of reference, and was eliminated if the deviation was not a part of a continuous path. Further, the source of inward error was independent of a radial bias commonly observed in simple, single-point tactile localisation tasks (Culver, 1970; Mancini et al., 2011).

Inward errors in tactile localisation suggest that computations analogous to path integration occur in the human somatosensory system (see also, Moscatelli et al., 2014, for a similar proposal in the case of tactile perception of shapes). Our methods cannot entirely exclude the possibility that participants transformed the spatial locations of the start and end points of the motion path into external spatial coordinates prior to bisecting them. However, this would not readily explain the consistent inward mislocalisation error. Instead, our findings support the idea that tactile localisation is influenced by the spatiotemporal pattern of skin stimulation within a spatially-organised representation of the array of tactile RFs covering the skin surface. This could correspond to a barycentric coordinate system, enabling the computation of tactile distance, without any transformation into external spatial coordinates.

A characteristic feature of early levels of cortical somatosensory processing is a topographically-organised map of skin locations, in which adjacent neurons typically receive afferent inputs from adjacent RFs on the skin (Mountcastle, 2005). However, the mere existence of ordered brain topography does not, by itself, imply that a cognitive map of the body surface is used for direct perception of absolute spatial location. Instead, additional mechanisms complementing the topographic organisation are necessary. Crucially, early theories suggested that the spatial quality of sensations was not based on direct perception of any spatial property, but derived from other non-spatial factors, such as visual cues or motor commands (e.g., saccades) required to make an

orienting response to the stimulated location (Banks, 2003; Halnan & Wright, 1960). However, voluntary orienting movements are arguably not the only foundation for the experience of spatial location. Indeed, displacements of a stimulus location might not be perceived during motion, as for example in the case of small displacements of a visual target during saccadic eye movements (Bridgeman, Hendry, & Stark, 1975; Deubel, Bridgeman, & Schneider, 2004) and in the case of small displacements of a tactile target during haptic movements (Ziat, Hayward, Chapman, Ernst, & Lenay, 2010). We suggest that the spatial quality of tactile percepts derives from experiencing patterns of stimulation traversing adjacent RFs. Patterns of natural motion, such as a spider crawling across the skin, or a twig brushing against an animal moving through a forest, typically stimulate a set of RFs in a specific spatiotemporal order. The temporal succession of signals reaching the brain from each RF establishes the *relative* positions of the RFs, establishing space from the temporal order of travel (Nicod, 1924). Mechanisms of Hebbian learning (Hebb, 1949), augmented by local interneuronal connections between cortical neurons (Gupta, Wang, & Markram, 2000; Laskin & Spencer, 1979), would allow such a system to learn local adjacency relations. The transition from one RF to its neighbour would allow the system to keep track of a continuously moving stimulus, and to perceive its current location relative to nearby stimulated locations. Tactile space perception could thus be based on computing relative position and motion information, analogous to the way that navigating animals construct a spatial map of the environment from self-motion cues (Etienne & Jeffery, 2004). Under this framework, computation of tactile distance depends upon the statistics of natural tactile stimuli. This is also conceptually similar to the observation that visual perception of length is shaped by the statistics of natural visual inputs (Howe & Purves, 2002).

This view can be compared with a previous interpretation suggesting that perception of somatosensory spatial properties (e.g., tactile stimulus location, shape and size) relies on an explicit model of the body, which encodes absolute position information (Longo, Azañón, & Haggard, 2010). These authors argued for a two-stage process of tactile localisation: first, the stimulus is localised relative to other positions within a somatotopic coordinate space covering a particular skin region, without reference to explicit models of the body or the world. Then, its relative somatotopic position is remapped onto an absolute location on the body surface via an explicit model of the body and its metric properties. When tracking a tactile stimulus moving across the skin, each successively stimulated skin location could either be referenced to an absolute location on a cognitive map of the body surface, or processed within a relative, RF-based coordinate space until such time as a response is required. Our bisection data is compatible with the latter view, namely, that the path of a moving tactile stimulus is traced by computations of relative positions and RF adjacency.

Our findings suggest the intriguing possibility that localisation on the skin involves similar neural processes to those underpinning navigation through the external environment. Previous functional magnetic resonance imaging (fMRI) studies showed that navigation in humans is mediated by a network of brain regions including hippocampal, parietal, temporal and prefrontal areas (Doeller et al., 2010). Parietal cortex represents space from an egocentric point of view in body-centred coordinates (Schindler & Bartels, 2013; Stein, 1989). In contrast, hippocampal neurons encode representation of allocentric spatial relations, i.e., a cognitive map of the environment, as initially suggested by seminal work on freely moving rats (O'Keefe & Dostrovsky, 1971). These representations are specifically enabled by neuronal populations known as place and grid cells (Moser, Kropff, & Moser, 2008). The environment-centred representations provided by these cells are constructed from self-motion cues, allowing the animal to represent location based on relative, rather than absolute position information. Our research raises the intriguing possibility that tactile RFs may serve as a grid that computes the position and motion of a stimulus. A tactile stimulus traversing adjacent RFs on the skin would be analogous to an

animal navigating across an environment, integrating self-motion cues and triggering firing in a succession of grid cells. We have argued that these computations may emerge from integration of successive stimulation of adjacent RFs.

One limitation of the present study is that we did not directly compare different computational mechanisms underlying tactile spatial perception or different path integration models. For example, we considered a fixed, grid-like arrangement of RFs, and did not take into account how factors such as RF overlap, size variation or hierarchical organisation could influence path integration. In principle, the computational mechanisms of local adjacency and succession that we describe should be relatively independent of such factors. However, we cannot exclude other neuroanatomical and functional principles that might support the ability to perceive spatiality on the skin surface.

Crucially, we based our reasoning on the assumption that the inward error is a marker of path integration. Although the inward error is a common observation in the navigation literature, different models regarding how direction and angle information is integrated have been proposed (Etienne & Jeffery, 2004; McNaughton, Battaglia, Jensen, Moser, & Moser, 2006; Müller & Wehner, 1988). Those models propose differing accounts of how the inward error comes about, and no consensus has been reached on that point. However, all these models agree that the inward error is key to the process of path integration.

The mechanism we describe cannot by itself explain all tactile spatial perception. For example, tactile path integration does not account for the ability to localise single points of tactile stimulation, nor for the ability to compute spatial relations between multiple discrete points of stimulation. Extensive experience of continuous natural motions across the skin may allow the brain to build up abstract representations of spatial location that support spatial perception without integration of continuous inputs.

In conclusion, the successive stimulation of adjacent RFs might underlie a RF-based mechanism of space perception. A mechanism of path integration could integrate the motion of a stimulus from one tactile RF to its neighbours, allowing a system of spatial representation based on cumulating relative positions. This mechanism would be similar to that which animals use to navigate in the environment, representing locations in terms of the self-motion cues required to move between them. In support of this view, we demonstrate that tactile localisation shows the same characteristic errors as navigation by path integration. We thus propose a RF-based, 'skin-space' mechanism of tactile localisation, based on three pillars: statistics of natural tactile inputs involving successive stimulation of adjacent RFs, a representation of RF adjacency, and path integration of a series of local vectors linking one stimulated RF to the next stimulated RF. Importantly, this model allows basic spatial representation of relative positions on the skin surface without any explicit models or cognitive maps of either the body or external egocentric space. Our evidence that tactile path integration shares similar behavioural characteristics with navigation by path integration paves the way for novel empirical questions about the computational and neuronal code underpinning the spatial perception of the body.

## Acknowledgements

PH acknowledges generous support from a donation by Shamil Chandaria to the School of Advanced Study. This research was further supported by ERC Advanced Grant HUMVOL (agreement number 323943). The article benefitted from a fellowship at the Paris Institute for Advanced Studies (France), with the financial support of the French State managed by the Agence Nationale de la Recherche, programme "Investissements d'avenir", (ANR-11-LABX-0027-01 Labex RFIEA+). FF was supported by EU FP7 Project VERE WP1. BB was supported by an MRC grant (number MR/M013901/1) to PH. The authors thank Colin Blakemore, GianDomenico Iannetti and Micah Allen for helpful discussions.

## Appendix A. Supplementary material

Supplementary data associated with this article can be found, in the online version, at <http://dx.doi.org/10.1016/j.cognition.2018.05.024>.

## References

- Banks, E. C. (2003). *Ernst Mach's world elements: A study in natural philosophy*. Dordrecht: Kluwer.
- Bridgeman, B., Hendry, D., & Stark, L. (1975). Failure to detect displacement of the visual world during saccadic eye movements. *Vision Research*, *15*(6), 719–722.
- Buonomano, D. V., & Merzenich, M. M. (1998). Cortical plasticity: From synapses to maps. *Annual Review of Neuroscience*, *21*, 149–186.
- Constantinescu, A. O., O'Reilly, J. X., & Behrens, T. E. J. (2016). Organizing conceptual knowledge in humans with a gridlike code. *Science*, *352*(6292), 1464–1468.
- Culver, C. M. (1970). Errors in tactile localization. *The American Journal of Psychology*, *83*(3), 420–427.
- Deubel, H., Bridgeman, B., & Schneider, W. X. (2004). Different effects of eyelid blinks and target blanking on saccadic suppression of displacement. *Perception & Psychophysics*, *66*(5), 772–778.
- Doeller, C. F., Barry, C., & Burgess, N. (2010). Evidence for grid cells in a human memory network. *Nature*, *463*(7281), 657–661.
- Etienne, A. S., & Jeffery, K. J. (2004). Path integration in mammals. *Hippocampus*, *14*(2), 180–192.
- Favorov, O. V., Diamond, M. E., & Whitsel, B. L. (1987). Evidence for a mosaic representation of the body surface in area 3b of the somatic cortex of cat. *Proceedings of the National Academy of Sciences*, *84*(18), 6606–6610.
- Gupta, A., Wang, Y., & Markram, H. (2000). Organizing principles for a diversity of GABAergic interneurons and dynapses in the neocortex. *Science*, *287*(5451), 273–278.
- Hafting, T., Fyhn, M., Molden, S., Moser, M.-B., & Moser, E. I. (2005). Microstructure of a spatial map in the entorhinal cortex. *Nature*, *436*(7052), 801–806.
- Halnan, C. R. E., & Wright, G. H. (1960). Tactile localization. *Brain*, *83*(4), 677–700.
- Hebb, D. O. (1949). *The organization of behavior: A neuropsychological theory*. New York: John Wiley and Sons.
- Howe, C. Q., & Purves, D. (2002). Range image statistics can explain the anomalous perception of length. *Proceedings of the National Academy of Sciences*, *99*(20), 13184–13188.
- Iwamura, Y., Iriki, A., & Tanaka, M. (1994). Bilateral hand representation in the post-central somatosensory cortex. *Nature*, *369*(6481), 554–556.
- Killian, N. J., Jutras, M. J., & Buffalo, E. A. (2012). A map of visual space in the primate entorhinal cortex. *Nature*, *491*(7426), 761–764.
- Laskin, S. E., & Spencer, W. A. (1979). Cutaneous masking. II. Geometry of excitatory and inhibitory receptive fields of single units in somatosensory cortex of the cat. *Journal of Neurophysiology*, *42*(4), 1061–1082.
- Longo, M. R., Azañón, E., & Haggard, P. (2010). More than skin deep: Body representation beyond primary somatosensory cortex. *Neuropsychologia*, *48*(3), 655–668.
- Longo, M. R., & Haggard, P. (2011). Weber's illusion and body shape: Anisotropy of tactile size perception on the hand. *Journal of Experimental Psychology: Human Perception and Performance*, *37*(3), 720–726.
- Lotze, H. (1884). *Mikrokosmos*. Leipzig: Hirzel.
- Mancini, F., Longo, M. R., Iannetti, G. D., & Haggard, P. (2011). A supramodal representation of the body surface. *Neuropsychologia*, *49*(5), 1194–1201.
- Margolis, A. N., & Longo, M. R. (2015). Visual detail about the body modulates tactile localisation biases. *Experimental Brain Research*, *233*(2), 351–358.
- McNaughton, B. L., Battaglia, F. P., Jensen, O., Moser, E. I., & Moser, M.-B. (2006). Path integration and the neural basis of the “cognitive map”. *Nature Reviews Neuroscience*, *7*(8), 663–678.
- Mittelstaedt, M.-L., & Mittelstaedt, H. (1980). Homing by path integration in a mammal. *Naturwissenschaften*, *67*(11), 566–567.
- Moscattelli, A., Naceri, A., & Ernst, M. O. (2014). Path integration in tactile perception of shapes. *Behavioural Brain Research*, *274*, 355–364.
- Moser, E. I., Kropff, E., & Moser, M.-B. (2008). Place cells, grid cells, and the brain's spatial representation system. *Annual Review of Neuroscience*, *31*(1), 69–89.
- Mountcastle, V. B. (2005). *The sensory hand: Neural mechanisms of somatic sensation*. Harvard University Press.
- Müller, M., & Wehner, R. (1988). Path integration in desert ants, *Cataglyphis fortis*. *Proceedings of the National Academy of Sciences*, *85*(14), 5287–5290.
- Nicod, J. (1924). *La géométrie dans le monde sensible*. Paris: Alcan.
- O'Keefe, J., & Dostrovsky, J. (1971). The hippocampus as a spatial map. Preliminary evidence from unit activity in the freely-moving rat. *Brain Research*, *34*(1), 171–175.
- Penfield, W., & Boldrey, E. (1937). Somatic motor and sensory representation in the cerebral cortex of man as studied by electrical stimulation. *Brain*, *60*(4), 389–443.
- Penfield, W., & Rasmussen, T. (1950). The cerebral cortex of man: A clinical study of localization of function. *Journal of the American Medical Association*, *144*(16), 1412–1412.
- Prokopenko, R. A. (2012). *Prok.Phantom*. Retrieved from < <http://sivirt.utsa.edu/Documents/Manuals/Prok-Phantom%20Manual.pdf> > .
- Rose, D. (1999). The historical roots of the theories of local signs and labelled lines. *Perception*, *28*(6), 675–685.
- Schindler, A., & Bartels, A. (2013). Parietal cortex codes for egocentric space beyond the field of view. *Current Biology*, *23*(2), 177–182.
- Schlereth, T., Magerl, W., & Treede, R.-D. (2001). Spatial discrimination thresholds for pain and touch in human hairy skin. *Pain*, *92*(1), 187–194.
- Stein, J. F. (1989). Representation of egocentric space in the posterior parietal cortex. *Quarterly Journal of Experimental Physiology*, *74*(5), 583–606.
- Yartsev, M. M., Witter, M. P., & Ulanovsky, N. (2011). Grid cells without theta oscillations in the entorhinal cortex of bats. *Nature*, *479*(7371), 103–107.
- Ziat, M., Hayward, V., Chapman, C. E., Ernst, M. O., & Lenay, C. (2010). Tactile suppression of displacement. *Experimental Brain Research*, *206*(3), 299–310.